

12-1-2013

Finite Element Analysis of FRP Debonding Failure at the Tip of Flexural/Shear Crack in Concrete Beam

Tayyebah Mohammadi
Marquette University

Baolin Wan
Marquette University, baolin.wan@marquette.edu

Kent Harries
University of Pittsburgh

FINITE ELEMENT ANALYSIS OF FRP DEBONDING FAILURE AT THE TIP OF FLEXURAL/SHEAR CRACK IN CONCRETE BEAM

T. Mohammadi¹, B. Wan² and K. Harries³

¹Department of Civil, Construction, and Environmental Engineering, Marquette University, USA.

²Department of Civil, Construction, and Environmental Engineering,
Marquette University, USA, Email: Baolin.Wan@marquette.edu.

³Department of Civil and Environmental Engineering, University of Pittsburgh, USA.

ABSTRACT

One of the most common failure modes of strengthened RC beams with externally bonded FRP is intermediate crack (IC) debonding of FRP initiated at the tip of flexural/shear cracks. This study presents a method, using extended finite element method (XFEM), to model IC debonding in an FRP-strengthened concrete beam. In XFEM, as soon as a damage initiation criterion is reached in an element, additional degrees of element freedom are added to model crack initiation. Crack propagation is then modeled using fracture energy criterion. This method can be used to simulate debonding failure along an arbitrary, solution-dependent path without the requirement of remeshing. The numerical results are validated against experimental data and good agreement is found. A sensitivity analysis is conducted to study the effects of damage band properties and geometry on FRP debonding failure. This verifies that shear strength and critical mode II fracture energy are the parameters most affecting the FRP debonding model when the crack tip is subjected to mode II loading.

KEYWORDS

FRP, concrete beams, XFEM, IC debonding, finite element.

INTRODUCTION

Carbon fiber reinforced polymer (CFRP) composite materials were first successfully used to retrofit a damaged bridge in Lucerne, Switzerland in 1991 (Meier 1995). Since then, externally bonded FRP for repair/strengthening of concrete structures has been widely adopted due to the good material properties of FRP for this application (Bakis *et al.* 2002; Teng *et al.* 2002; Bank 2006). Failure of FRP-strengthened reinforced concrete flexural members is often caused by debonding of FRP with a thin layer of concrete that is a sudden and brittle failure (Hollaway and Teng 2008; Oehlers and Seracino 2004). If there is sufficient anchorage at the end of FRP plates, the debonding failure generally begins at the tip of flexural/shear cracks and propagates along FRP/concrete interface toward the supports of the beam. This type of debonding failure is called intermediate crack-induced (IC) debonding failure and is shown schematically in Figure 1. This failure mode is not fully understood.

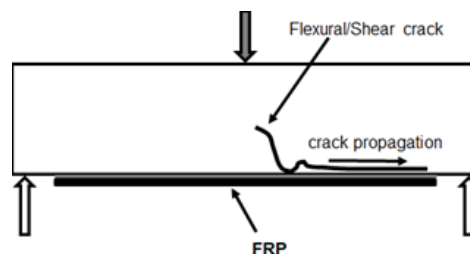


Figure 1. Typical intermediate crack (IC) debonding failure

In this paper, experimental tests conducted by Harries *et al.* (2012) are modelled numerically using the extended finite element method (XFEM). XFEM uses damage initiation and propagation criteria to model cracking in bulk material. In this method, a crack is initiated and then propagates along an arbitrary path within a damage

band instead of along a predefined surface as is the case using many other modelling methods. Therefore, XFEM is a more objective method. Comparison of numerical and experimental results shows that the applied method is able to model the IC debonding failure of FRP-strengthened beams. Parametric sensitivity analysis of the strengthened beams is then conducted to study the effects of damage band properties and geometry on FRP debonding failure.

FINITE ELEMENT ANALYSIS USING XFEM

Experimental Background

Harries *et al.* (2012) used notched three-point bending beam specimens, shown in Figure 2, for assessing FRP-to-concrete bond behaviour in FRP-strengthened beams. The specimen dimensions are similar to that used to determine the modulus of rupture of concrete (ASTM C78). The notch at mid-span, cut to one half of the beam depth, represents the cracked concrete beam. Three specimens (G3-A, B, and C) have been used for numerical modelling and analysis in the present study. In these specimens, the reported dimensions are: $h=b=L/3 = 152$ mm, $w = 75$ mm, FRP thickness = 1.9 mm, and $S = 380$ mm.

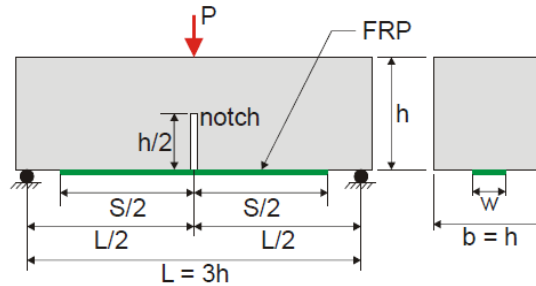


Figure 2. Test specimen (Harries *et al.* 2012)

Extended Finite Element Model (XFEM)

The extended finite element model (XFEM) can simulate the initiation and propagation of discontinuities (cracks) in finite element analysis by using additional degrees of freedom for the cracked elements. The failure mechanism is defined by a traction separation law in a damage band. The traction separation law includes a damage initiation criterion and a damage propagation criterion. In this study, a bilinear traction separation law is assumed to model the bond behaviour of the damaged area as shown in Figure 3. The damaged band is a defined area in which the crack most probably initiates and through which the crack most probably propagates. According to most experimental data, FRP debonding occurs in the concrete close to the concrete/FRP interface. Therefore, a damage band parallel to the FRP/concrete interface is assumed as shown in Figure 4. The traction separation law including damage initiation and propagation criteria is assigned to this area in order to model the debonding behaviour. An elliptic form, given in Eq. 1, defines the damage initiation criterion:

$$\left(\frac{\sigma}{\sigma_n}\right)^2 + \left(\frac{\tau}{\tau_s}\right)^2 = 1 \quad (1)$$

where σ_n , and τ_s are the normal and shear bond strengths of the damage band, respectively; and σ and τ are the normal and shear stresses of the element under applied loading, respectively.

A linear relationship is defined for the damage propagation criterion:

$$\frac{G}{G_C} = \left(\frac{G_I}{G_{IC}}\right) + \left(\frac{G_{II}}{G_{IIC}}\right) = 1 \quad (2)$$

where G_I and G_{II} are the strain energy release rate components of mode I and II, respectively; and G_{IC} and G_{IIC} are the critical strain energy release rates in pure mode I and II loadings, respectively.

The required damage band properties in Eqs 1 and 2 are: normal (mode I) bond strength, σ_n , critical mode I fracture energy, G_{IC} , shear (mode II) bond strength, τ_s , and critical mode II fracture energy, G_{IIC} . In this study, the properties of the damage band in the normal (mode I) direction (σ_n and G_{IC}) are assumed equal to those of substrate concrete, and the properties in the shear (mode II) direction (τ_s and G_{IIC}) are calculated to obtain the best agreement with experimental results. The material properties of the substrate concrete, GFRP plate, and adhesive used for the specimens and in the XFEM analysis are presented in Table 1.

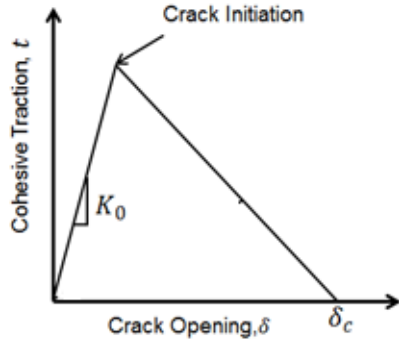


Figure 3. Bilinear traction separation law

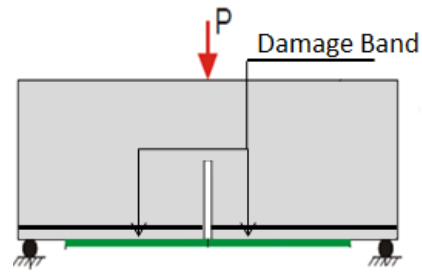


Figure 4. Damage band parallel to the concrete/FRP interface

Table 1. Material properties used in FEM

Material Property	Concrete	GFRP	Adhesive
Young's Modulus, E , (GPa)	26.1	41.37	1.2
Compressive Strength, f'_c , (MPa)	32	-	-
Tensile Strength, f'_t , (MPa)	3.5	-	-
Poisson Ratio, ν	0.25	0.2	0.3
Fracture Energy, G_F , (N/m)	150	-	-

Damage Band Shear Modulus

One of the controversial issues in defining the damaged band properties is how to determine the stiffness. Since it is assumed that cracking initiates and propagates in the substrate concrete, the Young's modulus of concrete can be assigned to the damage band. However, the shear modulus of this area is smaller than the concrete shear modulus because of the adhesive shear stiffness contribution to the shear stiffness of the damage band. The initial shear stiffness, k_0 in Figure 3, is less than $\frac{G_c}{t}$ of concrete according to Eq. 3 (Dai *et al.* 2005):

$$k_0 = \frac{G}{t} = \frac{1}{\frac{t_a}{G_a} + \frac{t_c}{G_c}} \quad (3)$$

where G_c , G_a , t_c , and t_a are the shear moduli, and the thicknesses of the concrete and adhesive, respectively.

Finite Element Results

Figure 5 shows the load versus FRP strain at midspan (immediately below the vertical notch in Figure 4) curves obtained from experimental data (Harries *et al.* 2012) and the numerical results from the present XFEM analyses. It can be seen that the XFEM method with the assumed material properties is able to predict the trend of the specimen behaviours and the debonding failure.

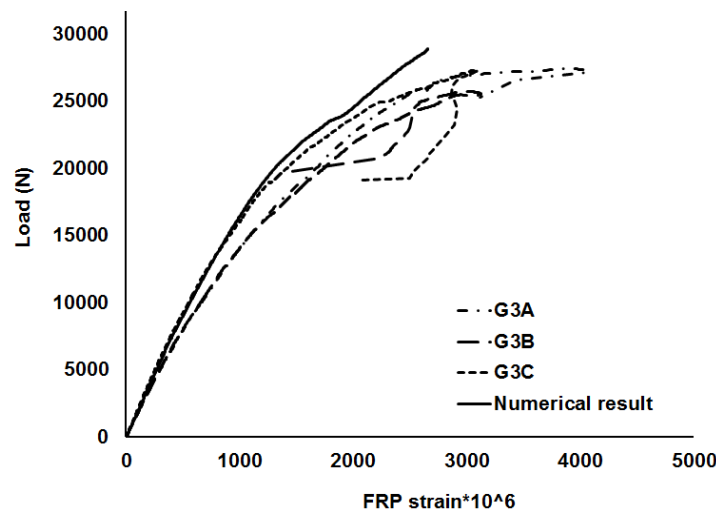


Figure 5. Numerical results against experimental results for load vs. FRP strain at midspan

The numerical results are virtually identical to the experimental data before the initiation of debonding. However, after cracking initiation, the numerical analysis predicts less FRP strain; that is, stiffer results compared with experiments. This is typical when modelling concrete structures. A larger ultimate capacity is predicted by the finite element analysis. It is indicated in Harries *et al.* (2012) that the failure of most of the specimens was characterized as an adhesive failure between the FRP and adhesive at lower loads than anticipated. This failure suggests improper preparation of the FRP strips or substrate prior to installation although had no influence on the objective of Harries *et al.* (2012). However, in the present numerical analysis, the FRP debonding is assumed to occur within the concrete substrate. This explains the larger ultimate capacity predicted by the numerical model.

SENSIVITY ANALYSIS

Since debonding failure typically controls the behaviour of FRP strengthened specimens, the damage band geometry and properties play an important role in the predicted failure behaviour. In this part of the study, the thickness and properties of the damage band are varied to study their effects on modeling the FRP debonding from concrete.

Sensitivity to Damage Band Properties

Typical flexural/shear cracks in the concrete substrate often cause a mixed-mode debonding behaviour, including both in-plane normal and shear stresses. Eqs 1 and 2 account for the contribution of mode I and mode II characteristics in FRP debonding failure.

The first sensitivity analysis investigates the effects of the mode I properties on the debonding failure. Figure 6 presents the results of analyses for beams with different normal bond strength, σ_n , and mode I critical fracture energy, G_{IC} . As can be seen, the numerical models are insensitive to the mode I properties even when they are reduced 50%. As a result, the mode I contribution does not have significant effect on debonding failure initiated at the tip of notch, when the notch is placed at the middle of the beam span.

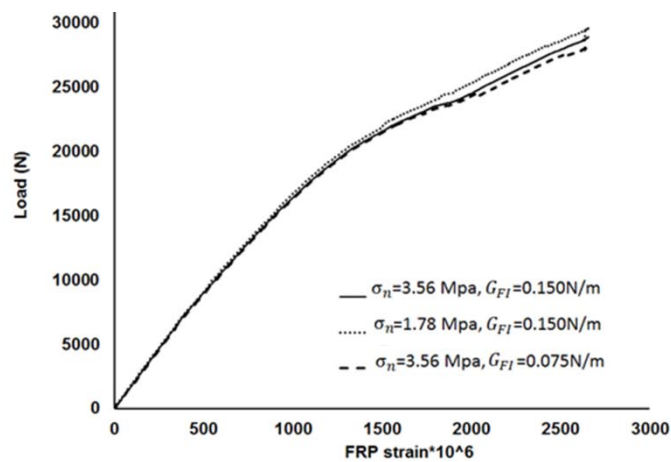


Figure 6. Sensitivity to the normal (mode I) properties

Figure 7 shows the sensitivity of the analyses to the mode II properties. The shear bond strength, τ_s , and mode II critical fracture energy, G_{IIC} are each changed 50%. As seen in the figure, mode II properties have a significant effect on the debonding behaviour and the results are very sensitive to these parameters. The ultimate load is significantly changed when τ_s and G_{IIC} are changed. Therefore, the FRP debonding initiated at the tip of a mid-span flexural crack is primarily controlled by mode II or shear properties. This also validates the test method proposed by Harries *et al.* (2012), which intends to test the FRP debonding due to mode II (in-plane shear) loading.

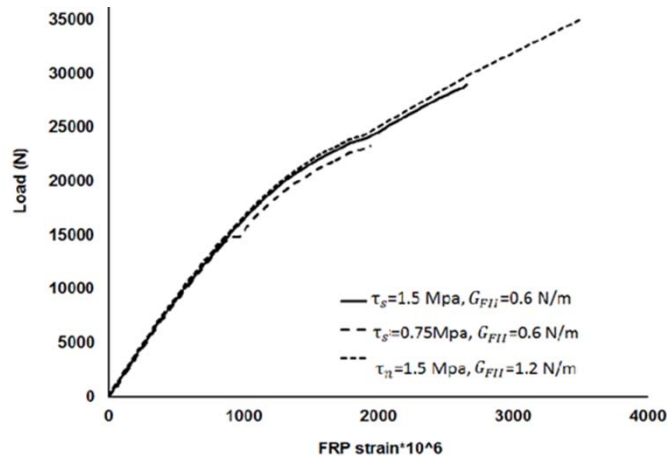


Figure 7. Sensitivity to the shear (mode II) properties

Sensitivity to Damage Band Thickness

In this section, the sensitivity of numerical results to the damage band thickness is considered. The finite element analysis is conducted with damage band thicknesses of 2, 4, and 10 mm. Numerically obtained load versus midspan FRP strain curves are shown in Figure 7. When the damage band thickness is increased from 2 mm to 10 mm (changed 500%), the decrease of the ultimate load is less than 10%. So the ultimate load is not very sensitive to the damage band thickness. However, a smaller damage band thickness results in stiffer behaviour. The damage band thickness of 10 mm gives the poorest prediction in comparison with the stiffness of the experimental curves; the results for 2 and 4 mm thicknesses are close to each other. This observation is compatible with the experimental observations that indicate the debonding and horizontal cracking generally occur 1 to 5 mm from the interface of concrete and adhesive.

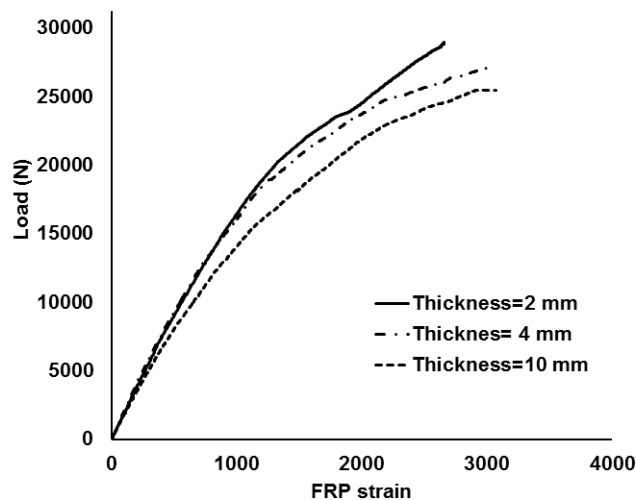


Figure 8. Sensitivity to the damage band thickness

CONCLUSION

In the present study, XFEM is successfully applied to model FRP debonding from a notched concrete beam. This method results in good agreement between numerical prediction and experimental observations. According to a sensitivity analysis, the shear (mode II) properties of the damage band including shear strength and critical fracture energy controls the FRP debonding initiated at the mid-span notch. The damage band thickness does not have a significant effect on the FRP debonding failure load. However, the damage band thickness affects the stiffness of the beam model. Damage band thicknesses of 2 to 4 mm give more compatible results in comparison with experimental observations.

ACKNOWLEDGMENTS

This study was supported by the financial aid for graduate student research assistant from Marquette University Graduate School.

REFERENCES

- Bakis, C.E. Bankmert, L.C. Brown V.L. Cosenza E. Davalos, J.F. and Lesko J.J. (2002). "Fiber-reinforced polymer composites for construction state-of-the art review", *Journal of Composites for Construction*, ASCE, 6(2), 73–87.
- Bank, L.C. (2006). "Composites for construction: structural design with FRP materials", *Chichester West Sussex, UK: John Wiley and Sons*.
- Dai, J. Ueda, T. Sato, and Y. (2005). "Development of the nonlinear bond stress-slip model of fiber reinforced plastics sheet-concrete interface with a simple methods", *journal of composites for construction*, 9(1),52-62.
- Harries, K. Hamilton, H.R. Kasan, J. and Tatar, J. (2012). Development of Standard Bond Capacity Test for FRP Bonded to Concrete", *6th international conference on Fiber Reinforced Polymer (FRP) Composites in Civil Engineering (CICE)*.
- Hollaway, L.C. Teng, J.G. (2008). "Strengthening and rehabilitation of civil infrastructures using fibre-reinforced polymer (FRP) composites", *Cambridge England: Woodhead Publishing Limited*.
- Meier, U. (1995). "Strengthening of structures using carbon fiber/epoxy composites", *Construction and Building Materials*, 9(6), 341-5.
- Oehlers, D.J. Seracino, R. (2004). Design of FRP and steel plated RC structures: retrofitting beams and slabs for strength, stiffness and ductility", *UK: Elsevier*.
- Teng, J.G. Chen, J.F. Smith, S.T. and Lam, L. (2002). "FRP strengthened RC structures", *UK: John Wiley and Sons*.